RSC Advances

PAPER

View Article Online
View Journal | View Issue

Cite this: *RSC Adv.*, 2016, **6**, 60138

Synthesis of photo-responsive azobenzene molecules with different hydrophobic chain length for controlling foam stability†

Shaoyu Chen, Chaoxia Wang,* Yunjie Yin and Kunlin Chen

Received 10th March 2016
Accepted 3rd June 2016

DOI: 10.1039/c6ra06459k

www.rsc.org/advances

To obtain an aqueous foam photo-switch, azobenzene molecules [4-hydroxy-4′-oxoalkyl azobenzene (HC_nAzo) n = 4, 8, and 12] were synthesized. The hydrophobic chain length affected both photo-responsive properties and foam stability controllability. *trans* → *cis* isomerization of HC_nAzo occurred by exposing to UV light for 1 s and the *cis* → *trans* process for HC_4Azo, HC_8Azo and HC_{12}Azo was carried out by visible light irradiation for 12 min, 13 min and 14 min, respectively. The reversible isomerization was repeatable, maintaining high sensitivity. Due to the small steric effect and isomerization barrier, photo-isomerization of HC_4Azo was more rapid than HC_8Azo and HC_{12}Azo. With the increase of the hydrophobic chain length, the decrease of thermal isomerization barrier resulted in less *cis* isomer and more *trans* isomer in photo-stationary state *via* UV and visible light irradiation, respectively. The combination of visible light and heat can accelerate the *cis* → *trans* isomerization speed. *trans* HC_4Azo, HC_8Azo and HC_{12}Azo increased foam life from 6.67 min to 10.38, 9.91 and 7.74 min, respectively, resulting from the absorption on the air–water interface and a high affinity. *cis* HC_4Azo, HC_8Azo and HC_{12}Azo decreased foam life from 6.67 min to 5.12, 5.49 and 6.02 min, respectively, attributed to the interfacial desorption and increase of surface tension. HC_4Azo with sensitive photo-isomerization and effective foam stability controllability was the best choice for an aqueous foam photo-switch.

Introduction

Foam, composed of gas bubbles and separated by thin liquid films, is a thermodynamically metastable system, which is widely used in the fine chemicals, petroleum chemicals, metallurgical mining, and food and textile industries.[1–3] The stability of foam is a crucial factor in its application. Surfactants, polymers and solid particles are usually used as foam stabilizers.[4–6] The role of the foam stabilizer is to slow down foam destabilization mechanisms, *i.e.*, drainage, coarsening and coalescence, by improving foam film strength or increasing viscosity.[7,8] Due to the large space occupation of residual foam, it is expected to be destroyed in a rapid and controlled way. Defoaming agents are usually used to break foam, but they are not a good choice for the reason that they prevent further re-foaming. Switchable foam is a new strategy to rapidly destroy residual foam and re-foam in a controllable way.[9]

Switchable foam is the ability of foam to be tuned by external stimuli such as pH,[10] CO_2, temperature, ionic strength, electricity, light, magnetic field, oxidants and enzymes.[11] Recently, light has attracted much attention to control the photo-responsive systems owing to its tunable parameters, including wavelength, intensity and duration.[12,13] In addition, a light trigger can be accurately localized, enabling both temporal and spatial control and is easily achieved using optical lenses, filters, and masks.[14,15]

Photosensitive chemicals contain a suitable chromophore whose surface activity changes upon UV-light irradiation. The chromophore can locate in the head group or tail chain of surfactant molecule, or even the connecting base of geminal surfactants. Typical chromophores are isomerization groups such as azobenzene and stilbene.[16] Azobenzene is very promising moiety due to its unique reversible photo-isomerization capability, high sensitivity and electrochemical activity.[17–19] Azobenzene derivatives have been proposed to utilize their *trans–cis* isomerization in energy storage, electronic devices and medical fields.[20–22] E. Chevallier *et al.*[23] reported a cationic azobenzene-containing surfactant. This surfactant can control stability and breakage of aqueous foam. However, the properties of cationic surfactants are easily affected by environmental factors such as electrolyte, which limits their field of application. For example, adhesive, as an indispensable agent in pigment dyeing and printing, is usually anionic. Therefore, the cationic azobenzene-containing surfactant cannot be applied in such a system. Compared to a cationic surfactant, a neutral molecule is more applicable. It can be compounded with all

Key Laboratory of Eco-Textile, Ministry of Education, School of Textile & Clothing, Jiangnan University, 1800 Lihu Road, Wuxi, 214122, People's Republic of China. E-mail: wangchaoxia@sohu.com

† Electronic supplementary information (ESI) available. See DOI: 10.1039/c6ra06459k

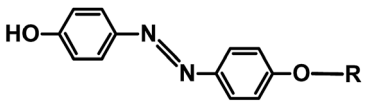

HC_4Azo: R = -C_4H_9
HC_8Azo: R = -C_8H_{17}
HC_{12}Azo: R = -$C_{12}H_{25}$

Fig. 1 Structure of azobenzene nonionic surfactants.

types of surfactants. However, the hydrophobic chain length of the neutral molecule influences its photo-response properties[24] and other properties, such as CMC value and solubility, which in turn affect the interface adsorption properties.

In this study, photo-responsive azobenzene molecules (HC_nAzo) were synthesized (as shown in Fig. 1) to optimize the hydrophobic chain length. They were synthesized with bromoalkane and 4,4′-dihydroxy azobenzene (DHAzo). The design of HC_nAzo was inspired from dodecanol, which possesses a superior foam stabilization capability.[25] HC_nAzo is expected to realize the quick switch between foam stabilizer and defoamer by alternating UV light and visible light irradiation, respectively. HC_nAzo characterization is performed with FT-IR, LC-MS and H-NMR analysis. The effects of raw materials, molar ratio and reaction time on yield are investigated for optimizing the synthesis process. Photo-isomerization speed and extent over a wide range of concentrations are investigated by UV absorption spectra. Influences of *trans* and *cis* isomers on foam stability and foamability are also investigated. HC_nAzo can tailor foam stability by light, which will show potential use in recycling residual foam to save chemical agents and decrease pollution.

Experimental

Materials

Potassium hydroxide (KOH, 99%), *p*-nitrophenol (99%), chlorohydric acid (HCl, 35%), diethyl ether (99%), ethanol (95%), potassium carbonate (K_2CO_3, 99%), bromododecane ($C_{12}H_{25}Br$, 98%), bromooctane ($C_8H_{17}Br$, 98%), bromobutane (C_4H_9Br, 98%), *N*,*N*-dimethylformamide (DMF, 99%), dichloromethane (CH_2Cl_2, 99%), petroleum ether (60–90 °C, 99%), ethyl acetate (99%), silica gel (FCP) and lauryl sodium sulfate (SDS, 99%) were purchased from Sinopharm Chemical Reagent Co., Ltd. Potassium iodide (KI, 99%) was obtained from Aladdin Industrial Inc. The water was deionized water.

Synthesis of HC_nAzo

HC_nAzo was synthesized *via* substituting the hydrogen atom of the OH group in DHAzo (homemade) with the alkyl group of the bromoalkane by the substitution reaction, as shown in Scheme 1.

Intermediate DHAzo. 100 g of KOH was dissolved and kept stirred in 20 mL of deionized water. 20 g of *p*-nitrophenol was introduced into the mixture of KOH and water. The reaction mixture was left to melt at 120 °C for 1 h and slowly heated to 200 °C. Then the reaction mixture was dissolved in water and adjusted to pH 3 with concentrated HCl solution. The product precipitated as a brown-yellow solid, which was extracted with diethyl ether after filtering. After evaporation, the precipitate was recrystallized in 50 : 50 v/v solution of ethanol/water to obtain a pure brownish-red crystalline product and finally dried under vacuum overnight. IR, ν/cm^{-1}: 3453, 3195, 1310–1410. ^{1}H NMR (400 MHz, CD_3OD) δ 6.92–6.94 (d, 4H), 7.77–7.79 (d, 4H).

Photo-responsive HC_nAzo. 6.35 g of DHAzo, 6.14 g of K_2CO_3 (1.5 eq.) and 0.5 g of KI were placed in 80 mL of DMF and stirred at 80 °C for 0.5 h. Then, the solution of bromoalkane and DMF was added dropwise to the reaction mixture and stirred at 80 °C for several hours. After reaction, the crude product was evaporated to remove DMF and then extracted with CH_2Cl_2. After removing CH_2Cl_2, the product was further purified with column chromatography (silica gel, petroleum ether/ethyl acetate, 7 : 1).

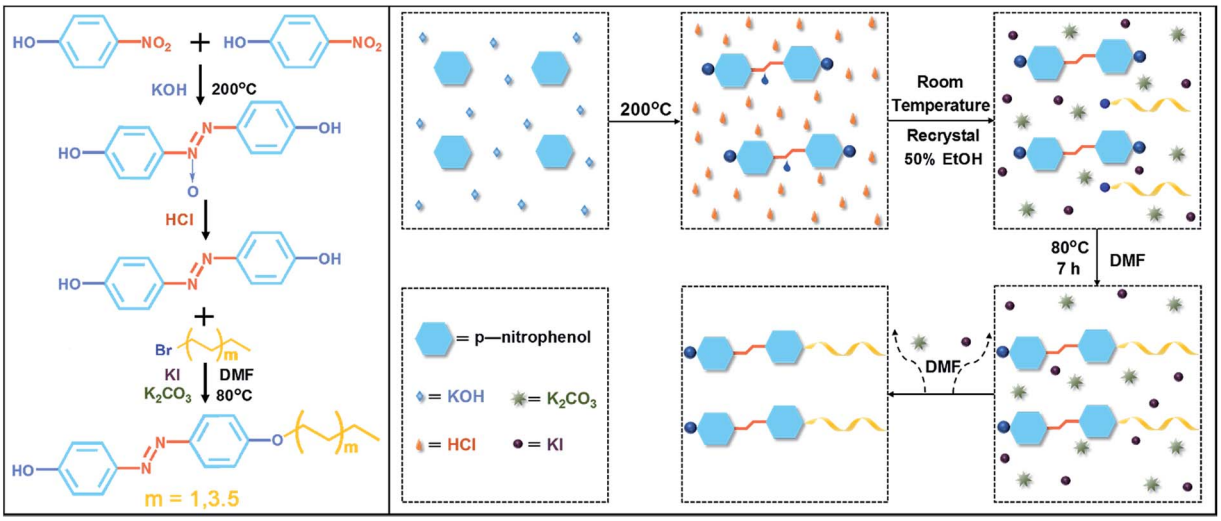

Scheme 1 Synthesis of HC_nAzo.

Characterization

Infrared spectra were obtained for solid samples on a Thermo Finnigan, Nicolet iS10, (USA) FT-IR spectrometer in KBr medium with the mass ratio of 1 : 100 to ensure uniform dispersion at ambient temperature. The mixed powders of the composites were pressed as clean discs. Liquid chromatography-mass spectrometry was recorded on a Thermo Finnigan, MALDI SYNAPT MS LC-MS (USA) spectrometer. The samples were dissolved in $CDCl_3$ and H-NMR spectroscopy was performed on a Bruker, Advance III 400 MHz spectrometer (Switzerland). The results are presented in the ESI.†

Isomerization monitoring

Isomerization of HC_nAzo was monitored with ultraviolet (UV) absorption spectra taken by a Cary 50 ultraviolet spectrophotometer. The ethyl acetate solutions of HC_nAzo (0.01 g L^{-1}, 0.02 g L^{-1} and 0.04 g L^{-1}) were exposed to UV light ($\lambda = 360$ nm, 175 mW cm^{-2}, Intelli-ray 600) and the change of their absorption spectra was monitored until the absorption maxima peak at 356 nm was constant, which meant reaching a *cis*-rich photo-stationary state. *cis* → *trans* reversible isomerization was monitored by irradiating with visible light (YG(B)982X, Wenzhou Darong Textile Instrument Co. Ltd., Zhejiang, China) and obtained absorption spectra until the disappeared absorption maxima peak re-emerged. A *trans*-rich photo-stationary state was obtained when the absorption spectra remained unchanged after prolonged visible light irradiation.

Calculation of isomeric compositions in photo-stationary states

The isomeric compositions in photo-stationary states represent the photo-isomerization extents, which are determined by spectrophotometry and calculated by eqn (1):[23]

$$\frac{A(\lambda)}{lC} = \tau\varepsilon_t + (1-\tau)\varepsilon_c \quad (1)$$

where $A(\lambda)$ is the absorbance at the wavelength λ, l is the length of the optical path, C is the concentration of HC_nAzo, ε_t and ε_c are the extinction coefficients of the *trans* and *cis* forms, respectively, and τ is the molar fraction of *trans* isomer. From absorbance of the all-*trans* and all-*cis* spectra, the extinction coefficients, ε_t and ε_c, were determined at the wavelength of 356 nm by eqn (1) with $\tau = 1$ and 0, respectively. The isomeric compositions of *trans* and *cis* in any other spectrum can thus be calculated by eqn (1) with the value of ε_t and ε_c. The samples of all-*trans* were kept in total darkness overnight prior to measurement and the all-*cis* samples were kept below 0 °C for 24 h before measurement so that the thermal reaction is frozen-out and one can assume that ε_c is temperature independent.[26,27]

Foam control properties analysis

Unless otherwise stated, solutions of HC_nAzo (0.01 g L^{-1}, 0.02 g L^{-1}, and 0.04 g L^{-1}, in ethyl acetate/water (v/v) = 1 : 10) were exposed under either UV or visible light before use. Under these conditions, the solutions reach a photo-stationary state containing either a *cis*-rich isomer or a *trans*-rich one. Foam was prepared from the dispersion containing HC_nAzo solutions and 2 g L^{-1} sodium dodecyl sulfate solution by stirring with a mixer (938A, Guangzhou Qihe Electrical Appliance Co., Ltd., Guangdong, China) for 2 min at room temperature. Foam stability was evaluated by foam life and drainage speed. Foam microscopy photographs were also used to evaluate foam properties, which were taken with a 10× USB digital microscope (AM801, Zhongshan Maisi Electronic Technology Co., Ltd., Guangdong, China).

Results and discussion

Isomerization analysis

In general, absorption spectroscopy can offer information about the structural characterization of the azobenzene derivatives owing to the transition moments of the azo group.[28] Fig. 2A–F shows the UV-Vis absorption spectra of HC_nAzo (0.01 g L^{-1}) revealing the photo-isomerization properties. Fig. 2A, C, and E show a strong $\pi \rightarrow \pi^*$ absorption peak at 356 nm and a weak $n \rightarrow \pi^*$ absorption peak at about 450 nm. Irradiation with UV light for only 1 s resulted in sufficient *trans*-to-*cis* photo-isomerization and a *cis*-rich photo-stationary state was reached, as evidenced by a prominent decrease in the absorbance at around 350–400 nm and a weak emergence in the $n \rightarrow \pi^*$ transition at 450 nm. Therefore, HC_nAzo were highly sensitive to UV light. On the other hand, Fig. 2B, D, and F show the opposite phenomenon indicating the reversible photo-isomerization (*cis*-to-*trans*) by visible light irradiation. In addition, as shown in Fig. 3A–C, the HC_nAzo photo-isomerization is reversible and it maintains the high sensitivity after repeating the photo-isomerization 20 times.

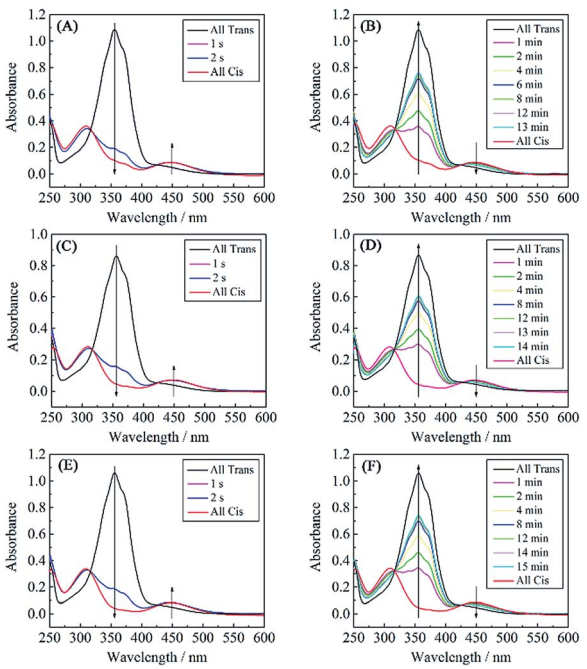

Fig. 2 Photo-isomerization of HC_nAzo at concentration of 0.01 g L^{-1} in UV light and visible light: (A) and (B) HC_4Azo, (C) and (D) HC_8Azo and (E) and (F) HC_{12}Azo.

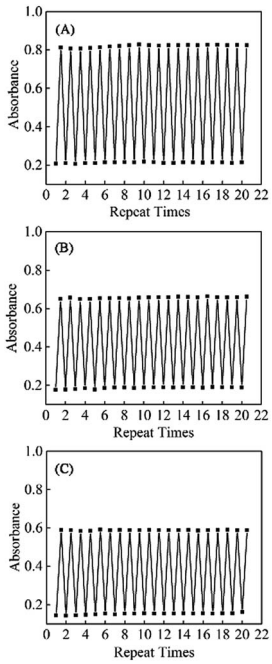

Fig. 3 Repeat times of HC_nAzo photo-isomerization at a concentration of 0.01 g L^{-1}. (A) Absorbance of HC_4Azo after exposing to UV light for 1 s (low absorbance) and visible light for 12 min (high absorbance). (B) Absorbance of HC_8Azo after exposing to UV light for 1 s (low absorbance) and visible light for 13 min (high absorbance). (C) Absorbance of $HC_{12}Azo$ after exposing to UV light for 1 s (low absorbance) and visible light for 14 min (high absorbance).

Because HC_nAzo is an azobenzene derivative (Abs), its photo-isomerization mechanism can be learned from azobenzene (AB). It is well known that AB exists in two different configurations (*trans* and *cis*) in S_0 (the electronic ground) state. According to some experimental results,[29] t-AB isomerization always occurs by UV light, which is in the S_1 (n–π*) state by an inversion process regardless of the initial excitation. Rotation contributes significantly in non-viscous media following $S_1 \leftarrow S_0$ excitation. Furthermore, c-AB undergoes photo-isomerization by rotation and thermal isomerization by inversion (shown in Fig. 4); therefore, it can occur not only by visible light irradiation, but also thermally in the dark.

However, substituents affect Abs isomerization through steric and electronic effects.[29] As for HC_nAzo, the electron-donating substituents (*i.e.* hydroxyl and alkoxy) cause a modest decrease in the thermal isomerization barrier by increasing the electron density in the π* orbital; therefore, it has higher rates of *cis* → *trans* thermal isomerization than AB. In the *trans* → *cis* isomerization process, S_1 and S_2 states are generated by *trans* isomers excitation. $S_1 \leftarrow S_0$ excitation occurs along the rotation pathway. Following $S_2 \leftarrow S_0$ excitation, the S_2 state rapidly relaxes to the S_1 state along the rotation pathway as the primary isomerization mechanism and then the S_1 state relaxes to the S_0 state.[29,30]

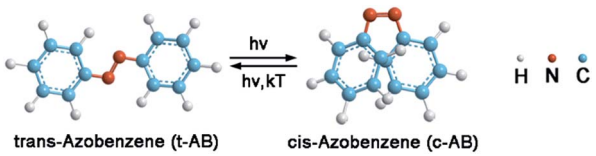

Fig. 4 Isomerization of AB.

As displayed in Fig. 2, *trans* → *cis* photo-isomerizations are rapid by exposing to UV light regardless of hydrophobic chain length. However, the *cis* → *trans* photo-isomerization speed slowed down upon increasing the hydrophobic chain length, which was consistent with the results reported by Hayashita.[24] The reason was that with the increase of the hydrophobic chain length, greater steric hindrance caused the inversion transition state to be higher in energy. On the other hand, increasing the hydrophobic chain length enhanced the electron-donating effect. This raised the inversion barrier height, making it harder to isomerize.[30] In addition to the photo-isomerization speed of HC_nAzo, the molar fractions of *cis* and *trans* isomer, representing the isomerization extent, in the photo-stationary state were calculated with the absorbance values in Fig. 2 and given in Table 1.

According to the results presented above, the *cis* isomer fraction decreased from 91.7% to 86.0% with the increase of hydrophobic chain length in the *cis*-rich photo-stationary state by UV light irradiation, while the *trans* isomer fraction showed a reverse trend in the *trans*-rich photo-stationary state by visible light irradiation. The increase of hydrophobic chain length enhanced the electron donating effect, which resulted in the decrease of thermal isomerization barrier in the *cis* to *trans* isomerization process. The *cis* isomer was easier to transform into the *trans* isomer by thermal isomerization, leading to the decrease of *cis* isomer fraction.

Fig. 5A–C present the comparison of photo-isomerization speed between different HC_nAzo concentrations. It shows that the photo-isomerization speeds slow down upon increasing HC_nAzo concentration regardless of hydrophobic chain length. This is because the photo-isomerization speed is decided by the photo-conversion of the bulk solution. With the increase of concentration, the solutions possessed higher absorbance in which the photo-conversion speed was very slow.[31] In addition, in a dilute HC_nAzo solution, the surfactant molecules exist in a monomer molecular state, whereas further increase of the surfactant concentration caused the formation of aggregations and micelles.[24] The photo-isomerization process occurred much more easily in the monomer molecular state than in the aggregated state.

cis to *trans* photo-isomerization was a little slow due to its higher excitation energies compared to *trans* isomers. It was more dependent on the structure and concentration of HC_n-Azo.[30] Since *cis* → *trans* photo-isomerization can occur not only

Table 1 *trans* and *cis* isomer molar fraction of HC_nAzo

Molar fraction	HC_4Azo	HC_8Azo	$HC_{12}Azo$
cis isomer (UV light)	91.7%	86.2%	86.0%
trans isomer (Vis light)	66.3%	68.6%	68.8%

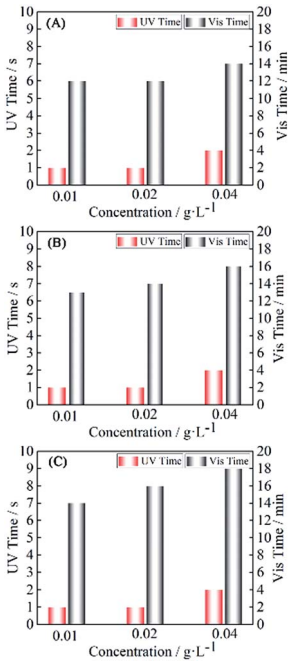

Fig. 5 Effects of HC_nAzo concentration on photo-isomerization speed: (A) HC_4Azo, (B) HC_8Azo and (C) $HC_{12}Azo$.

by visible light irradiation but also by thermal stimulation, it is predictable that *cis* → *trans* photo-isomerization speed can accelerate by supplementing thermal stimulation. Therefore, the *cis* → *trans* photo-isomerization processes of HC_4Azo were monitored at varied temperatures by UV-Vis absorption spectra, followed by calculating the *trans* isomer fractions. As shown in Fig. 6, it can be observed that as the temperature increases from 20 °C to 30 °C and 40 °C, the *cis* → *trans* photo-isomerization time decreases from 12 min to 6 min and then 5 min, respectively. The results indicated that the *cis* to *trans* isomerization speed is significantly increased by a combination of visible light irradiation and thermal stimulation in an appropriate temperature range (30 °C for 0.01 g L^{-1} of HC_4Azo in ethyl acetate solution). Over the temperature range, there was no obvious acceleration for *cis* to *trans* isomerization by further increasing the temperature. The *cis* to *trans* isomerization time is enough for recycling residual foam in common dyeing and finishing processes as most of these processes generally take at least 30 min.

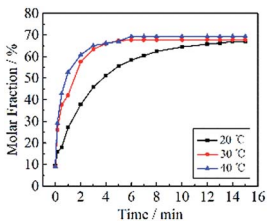

Fig. 6 Effects of temperature on *cis* → *trans* photo-isomerization speed (0.01 g L^{-1} of HC_4Azo).

Foam control properties

As illustrated in Fig. 7, each of HC_4Azo, HC_8Azo and $HC_{12}Azo$ can modulate foam stability over a wide range of concentrations. For instance, foam life increased from 6.67 min to 10.38 min in *trans*-rich HC_4Azo, while it decreased from 6.67 min to 5.12 min in *cis*-rich HC_4Azo at the concentration of 0.04 g L^{-1}. Therefore, it seemed that *trans* isomers showed a foam stabilization effect, and *cis* isomers accelerated rupture of the foam. In order to further confirm the stabilization effects of *trans* isomers, the life of foam which was prepared from the bulk and exposed to visible light for various times was measured. The *trans* isomer fraction gradually increased with prolonging visible light irradiation. As shown in Fig. 8, the foam life increases with a longer visible light irradiation. The *trans* isomers can thus be proven to have the capability to stabilize foam.

The interfacial adsorption of *trans* isomers can explain the stabilization of the foam. The *trans* isomer exhibited a high affinity, having π stacking forces in a face-to-face arrangement of azobenzene rings, which led to the formation of a nematic phase.[31,32] The strong attractive interaction caused the molecules of *trans* isomers reorient parallel to maintain planarity, resulting in the improvement of foam stability. In contrast, the destabilization of the *cis* isomers was mainly attributed to the interfacial desorption properties. The desorption constant of the *cis* isomers was higher than that of the *trans* isomers.[23] The *trans* isomers converted into *cis* isomers and rapidly desorbed from the interface when the *trans*-rich interface was exposed to UV light. The significant desorption resulted in a rapid increase of the surface tension and a weakening of the protection of the thin liquid films against coalescence.[31] In addition, non-homogeneous light irradiation intensities led to a gradient of

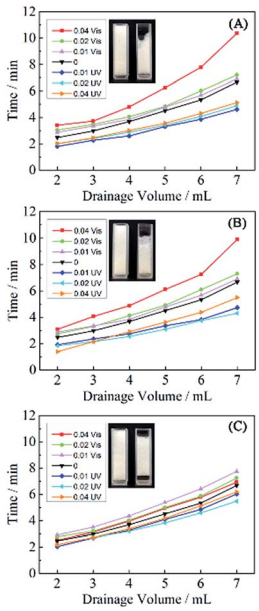

Fig. 7 Drainage volume dependence on time of foams stabilized at different concentrations of HC_nAzo: (A) HC_4Azo, (B) HC_8Azo and (C) $HC_{12}Azo$.

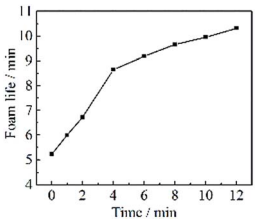

Fig. 8 Effects of visible light irradiation time on foam life (0.04 g L^{-1} of HC_4Azo and 2 g L^{-1} of SDS).

surface tension, resulting in Marangoni flows and accelerated liquid drainage. The irregular and random structure of the *cis* isomer without specific molecular interactions occupied a higher surface area, resulting in a rapid decrease of the surface excess. Interfacial adsorption/desorption properties of *trans* and *cis* $HC_{12}Azo$ made it possible to modulate foam stability.

Fig. 7A–C also shows effects of hydrophobic chain length of HC_nAzo on controllability of foam stability, which were dependent on its concentration. When the concentration was less than 0.01 g L^{-1}, $HC_{12}Azo$ showed the best foam control properties among HC_4Azo, HC_8Azo and $HC_{12}Azo$. The reason was that the *trans* isomer fraction of $HC_{12}Azo$ was higher than HC_4Azo and HC_8Azo in photo-stationary state. In addition, the longer hydrophobic chain length increased the affinity between *trans* isomers and the affinity of *trans* isomer and SDS (foaming agent). The foam film strength was increased, thereby increasing foam stability. However, HC_4Azo showed much more superior foam stability and controllability by further increase of the surfactant concentration. This was attributed to several factors such as CMC value and solubility. According to the report,[24] the CMC value decreased as the hydrophobic chain length increased. This meant that HC_nAzo, with longer hydrophobic chain length, was easier to aggregate at the same concentration and thus the number of monomer molecules adsorbed on the air/liquid interface was decreased. In addition, the solubility also decreased as the hydrophobic chain length increased. Due to the limit of solubility, the total number of soluble $HC_{12}Azo$ molecules in the bulk solution was not increased with increasing concentration. Moreover, the insoluble $HC_{12}Azo$ particles covered in the air/liquid interface or dispersed in the foam film, aggravating foam instability.

The effects of SDS concentration on foam life were investigated to prove that the foam control properties solely depended

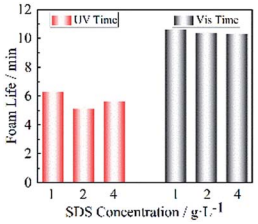

Fig. 9 Effects of SDS concentration on foam life (0.04 g L^{-1} of HC_4Azo).

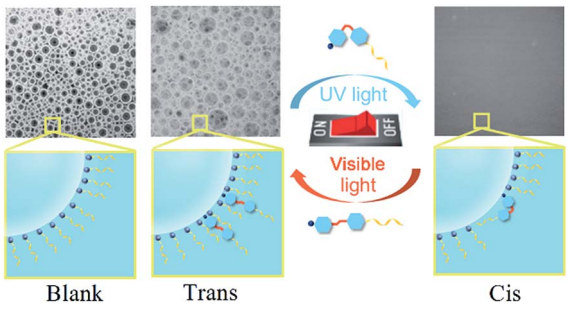

Fig. 10 Comparison of foam microscopy images and foam control mechanism (the images were taken after foaming for 5 min in 0.04 g L^{-1} of HC_4Azo).

on HC_nAzo. The results are displayed in Fig. 9. It was obvious that the foam life showed no significant change with the increase of SDS concentration, which indicated that the foam control properties only resulted from the transformation of HC_4Azo between *trans* and *cis* isomers. Because the ionic strength was determined by SDS concentration in this investigation, the results demonstrated that the ionic strength in solution presented no influence on the isomerization process.

Foam morphology was further investigated. As shown in Fig. 10, the comparison of foam morphology showed that foam with *trans*-rich HC_4Azo was more uniform and dense after foaming for 5 min. Before photo-isomerization, *trans* HC_nAzo adsorbed on foam air/water interface both in an orderly manner and densely, which can dramatically enhance the strength of the foam film. On the contrary, the *cis* isomer of HC_nAzo desorbed from the air/water interface, leading to an increase in the surface tension and the decrease of surface excess. Moreover, the increase of the steric hindrance resulted in more loose packing of HC_nAzo in the foam film. Therefore, the *cis* isomer of HC_nAzo made the foam ruptures quickly. It was realizable to prepare switchable foam by alternating the illumination with UV and visible light.

Conclusions

Azobenzene molecules HC_nAzo were synthesized and applied in aqueous foam to control foam stability. From the UV-Vis absorption spectra, HC_nAzo showed highly sensitive photo-response in UV light (1 s for *trans* → *cis* isomerization) regardless of the hydrophobic chain length, and in visible light, the *cis* → *trans* photo-isomerization time was increased upon increasing the hydrophobic chain length (*i.e.* 12, 13, 14 min for *cis* → *trans* isomerization of HC_4Azo, HC_8Azo and $HC_{12}Azo$, respectively). The increase of the hydrophobic chain length enhanced the electron-donating and steric effects, which increase the isomerization barrier, making the isomerization process slow. In addition, the enhanced electron-donating effect decreases the thermal isomerization barrier, resulting in less *cis* isomer and more *trans* isomer in photo-stationary state *via* UV and visible light irradiation, respectively. The *cis* → *trans* isomerization speed was accelerated by the combination of visible light and heat. Due to the adsorption properties,

trans HC_4Azo, HC_8Azo and HC_{12}Azo increased foam life from 6.67 min to 10.38, 9.91 and 7.74 min, respectively. In contrast, *cis* HC_4Azo, HC_8Azo and HC_{12}Azo decreased foam life from 6.67 min to 5.12, 5.49 and 6.02 min, respectively. In consideration of the photo-isomerization speed and foam stability controllability, HC_4Azo was considered as the most appropriate structure for obtaining a switchable foam. It is expected to tailor foam stability and recycle residual foam in textile foam dyeing and finishing, which will decrease water consumption and chemical pollution. The improvement of HC_4Azo solubility will be investigated in further study.

Acknowledgements

The authors are grateful for the financial support of the National Natural Science Foundation of China (21174055) and the Priority Academic Program Development of Jiangsu Higher Education Institutions.

References

1 A. Astarita, L. Carrino, S. Franchitti, A. Langella and V. Paradiso, *Surf. Interface Anal.*, 2013, **45**, 1638–1642.
2 C. Stubenrauch, L. K. Shrestha, D. Varade, I. Johansson, G. Olanya, K. Aramaki and P. Claesson, *Soft Matter*, 2009, **5**, 3070–3080.
3 H. Yu, Y. Wang, Y. Zhong, Z. Mao and S. Tan, *Color. Technol.*, 2014, **130**, 266–272.
4 Z. Du, M. P. Bilbao-Montoya, B. P. Binks, E. Dickinson, R. Ettelaie and B. S. Murray, *Langmuir*, 2003, **19**, 3106–3108.
5 L. K. Shrestha, E. Saito, R. G. Shrestha, H. Kato, Y. Takase and K. Aramaki, *Colloids Surf., A*, 2007, **293**, 262–271.
6 X. W. Song, L. Zhang, X. C. Wang, L. Zhang, S. Zhao and J. Y. Yu, *J. Dispersion Sci. Technol.*, 2011, **32**, 247–253.
7 E. Dickinson, R. Ettelaie, T. Kostakis and B. S. Murray, *Langmuir*, 2004, **20**, 8517–8525.
8 D. Georgieva, A. Cagna and D. Langevin, *Soft Matter*, 2009, **5**, 2063–2071.
9 A. L. Fameau, A. Carl, A. Saint-Jalmes and R. Von Klitzing, *ChemPhysChem*, 2015, **16**, 66–75.
10 Z. Chu and Y. Feng, *Chem. Commun.*, 2010, **46**, 9028–9030.
11 P. Brown, C. P. Butts and J. Eastoe, *Soft Matter*, 2013, **9**, 2365–2374.
12 S. Peng, Q. Guo, T. C. Hughes and P. G. Hartley, *Langmuir*, 2013, **30**, 866–872.
13 Y. Zhao, *Macromolecules*, 2012, **45**, 3647–3657.
14 B. A. Cicciarelli, T. A. Hatton and K. A. Smith, *Langmuir*, 2007, **23**, 4753–4764.
15 J. M. Schumers, C. A. Fustin and J. F. Gohy, *Macromol. Rapid Commun.*, 2010, **31**, 1588–1607.
16 J. Eastoe, M. S. Dominguez, P. Wyatt, A. Beeby and R. K. Heenan, *Langmuir*, 2002, **18**, 7837–7844.
17 C. L. Feng, G. Qu, Y. Song, L. Jiang and D. Zhu, *Surf. Interface Anal.*, 2006, **38**, 1343–1347.
18 A. Housni, Y. Zhao and Y. Zhao, *Langmuir*, 2010, **26**, 12366–12370.
19 X. Zhang, Y. Feng, P. Lv, Y. Shen and W. Feng, *Langmuir*, 2010, **26**, 18508–18511.
20 G. Abellán, H. García, C. J. Gómez-García and A. Ribera, *J. Photochem. Photobiol., A*, 2011, **217**, 157–163.
21 V. Ferri, M. Elbing, G. Pace, M. D. Dickey, M. Zharnikov, P. Samorì, M. Mayor and M. A. Rampi, *Angew. Chem.*, 2008, **120**, 3455–3457.
22 J. Liu, J. Nie, Y. Zhao and Y. He, *J. Photochem. Photobiol., A*, 2010, **211**, 20–25.
23 E. Chevallier, C. Monteux, F. Lequeux and C. Tribet, *Langmuir*, 2012, **28**, 2308–2312.
24 T. Hayashita, T. Kurosawa, T. Miyata, K. Tanaka and M. Igawa, *Colloid Polym. Sci.*, 1994, **272**, 1611–1619.
25 J. Wang, A. V. Nguyen and S. Farrokhpay, *Colloids Surf., A*, 2016, **488**, 70–81.
26 H. Rau, G. Greiner, G. Gauglitz and H. Meier, *J. Phys. Chem.*, 1990, **94**, 6523–6524.
27 A. D. Price, J. Ignés-Mullol, M. À. Vallvé, T. E. Furtak, Y. A. Lo, S. M. Malone and D. K. Schwartz, *Soft Matter*, 2009, **5**, 2252–2260.
28 C. L. Feng, J. Jin, Y. J. Zhang, Y. L. Song, L. Y. Xie, G. R. Qu, Y. Xu and L. Jiang, *Surf. Interface Anal.*, 2001, **32**, 121–124.
29 H. D. Bandara and S. C. Burdette, *Chem. Soc. Rev.*, 2012, **41**, 1809–1825.
30 C. R. Crecca and A. E. Roitberg, *J. Phys. Chem. A*, 2006, **110**, 8188–8203.
31 E. Chevallier, A. Mamane, H. Stone, C. Tribet, F. Lequeux and C. Monteux, *Soft Matter*, 2011, **7**, 7866–7874.
32 K. S. Yim and G. G. Fuller, *Phys. Rev. E*, 2003, **67**, 1601.

